Electromagnetic properties of model vitreous carbon foams

M. Letellier, J. Macutkevic, P. Kuzhir, J. Banys, V. Fierro, A. Celzard

Electromagnetic properties of model vitreous carbon foams

M. Letellier[1], J. Macutkevic[2], P. Kuzhir[3,4],

J. Banys[2], V. Fierro[1], A. Celzard[1*]

[1] Institut Jean Lamour, UMR CNRS – Université de Lorraine n°7198. ENSTIB, 27 rue Philippe Séguin, BP 21042, 88051 Epinal cedex 9, France

[2] Faculty of Physics, Radiophysics Department, Vilnius University, Sauletekio 9/3, 10022 Vilnius, Lithuania

[3] Institute for Nuclear Problems, Belarusian State University, 220030 Minsk, Belarus

[4] Tomsk State University, 36, Lenin Avenue, Tomsk, 634050, Russia

[*] Corresponding author. Tel: + 33 372 74 96 14. Fax: + 33 372 74 96 38. E-mail address : Alain.Celzard@univ-lorraine.fr (A. Celzard)

Abstract

This paper addresses the relationship between structural and electromagnetic (EM) properties of model vitreous carbon foams, i.e., presenting different porous structures in terms of bulk density, cell size and connectivity, while having the same composition and the same carbon texture. EM properties were investigated over a wide frequency range, from 20 Hz up to 250 THz. The bulk density is the main parameter controlling the EM behaviour up to ~ 50 GHz, as no change was found by varying other structural parameters such as cell size or interconnectivity in such frequency range. At low frequency, foams behave similarly to metals and, when the density increases, the reflection increases and the absorption decreases. The behaviour changes above ~ 50 GHz, absorption becoming the main mechanism. For cellular foams, transmission and reflection tend to be negligible in the infrared region, and behave like black bodies. However, reticulated foams present non-negligible transmission that increases with cell size. Resonance phenomena were observed for reticulated foams between about 0.2 and 3 THz. A simple model considering the fundamental mode TE_{10} of a rectangular waveguide whose largest dimension was the average cell diameter was proposed to predict minima and maxima of these resonances.

1. Introduction

This article is part of a large experimental study dealing with the physical properties of model vitreous carbon foams as a function of their porous structure. These materials are all made of the same vitreous carbon as evidenced in [1], and present very different bulk densities and cell sizes which are not correlated with each other. These special features allow for the first time accurate studies of physical properties of carbon foams as a function of their porous structure, hence the name "model foams" they were given. Mechanical and acoustic properties were already analysed in [2] and [3], respectively. Since these foams are made of vitreous carbon, they are electrically conducting. The electromagnetic (EM) properties of those carbon foams with very different structures were then thoroughly investigated here, in a very broad frequency range.

Details of the preparation and of the in-depth physicochemical and structural characterisation of the present model vitreous carbon foams have been extensively given in our former papers [1,2]. In the latter, more than 62 kinds of carbon foams, obtained through the preparation of 16 different types of formulations, were presented. Most of them were cellular vitreous carbon (CVC) foams, i.e., presenting more or less spherical cells connected with each other through more or less open (i.e., perforated) cell walls. In the following, such openings between cells are called "windows" (see Fig. 1). In addition, other carbon foams were prepared by resin templating of polyurethane foams, and were therefore called reticulated vitreous carbon (RVC) foams. Examples of CVC and RVC foams are presented in Fig. 2, in which the difference of porous structure can be easily seen.

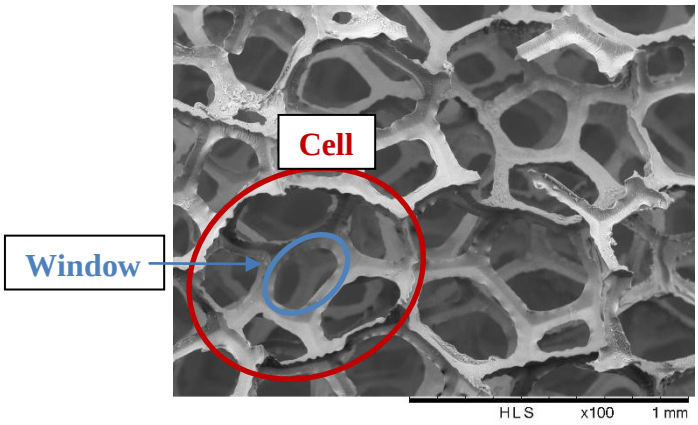

Fig. 1. Schematic structure of a reticulated carbon foam, emphasising the difference between cells and windows (i.e., holes connecting the cells).

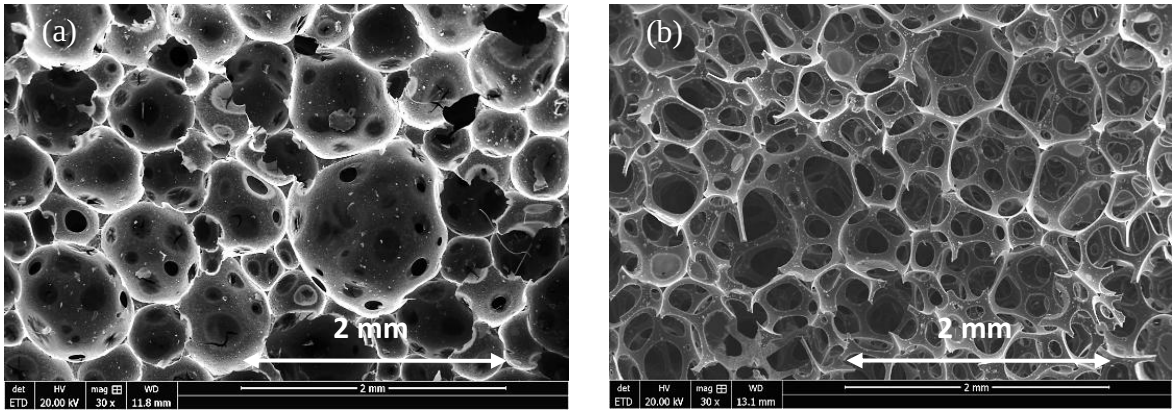

Fig. 2. Typical SEM pictures of: (a) CVC foam (formulation PPPT; density 0.094 g cm^{-3}), and (b) RVC foam (formulation RT, density 0.043 g cm^{-3}).

Several studies have been published about EM properties of porous media and foams [4–18]. This is a rather recent topic, and the interest is growing due to the exponential use of electronics in our everyday life. Indeed, materials such as carbon foams can be used for electromagnetic interference (EMI) shielding, either for protecting instruments from interferences that may come from outdoor, or for avoiding electromagnetic emissions from electric appliances. Composites mainly based on carbon nanotubes in a polymer matrix are widely studied for this type of applications, but carbon foams were found to have much higher

conductivities [5], strong EMI shielding in the microwave range, and high dielectric losses in the radiofrequency range [10,11,13]. Various studies also showed that the EM properties of these carbon foams can be optimised by modifying their structure [5,13].

In [4-6], tannin-based carbon foams of different densities (and cell sizes) were analysed from 20 Hz to 37 GHz. In the following, those materials were called "standard CVC foams"; their cell size increased when the bulk density decreased [19,20], just as in most other rigid foams. Their properties were compared with those of the present model carbon foams, i.e., having controlled cell size at a given density, or vice-versa, unlike the former "standard CVC foams".

For standard CVC foams, both dielectric permittivity [4,6] and electrical conductivity [4,21] in the quasi-static regime were high and increased with bulk density according to power laws. Significant electromagnetic interference shielding efficiency (*EMI SE*) was also found at microwave frequencies for all produced samples, and EMI shielding was shown to increase with density (which was always correlated with the decrease of cell size for these foams). The DC conductivity, analysed between -248 and +227°C, decreased with temperature according to Mott's law during cooling but the carbon foams still remained opaque to the microwave radiations. Moreover, it was shown [8] that two approaches can be used to model the EM properties of these foams in the microwave range, either based on a homogenisation procedure and considering the foam as a single layer of homogeneous conductive material, or considering the carbon foam as an analogue of photonic crystal with dielectric losses.

The EM properties of carbon foams can be controlled mainly through their density (or porosity) and the nature of the constituting carbon. The cell size, which is small compared to the wavelength in the microwave domain, does not seem to have any noticeable effect according to [12], but because density and cell size were always correlated with each other so

far, this finding should be confirmed. The EM properties of carbon foams can also be further improved by other methods such as filling the cells with CNTs – polymer composite [15] or by impregnation / deposition of magnetic or dielectric nanoparticles on the surface of the cells [22]. Finally, it should be noticed that carbon foams are already used in applications such as high-temperature insulation for aerospace vehicles where EMI shielding is also of great interest [16].

Thus, so far, the influences of bulk density, cell size and connectivity on the EM properties of carbon foams have never been investigated separately. The present work is thus devoted to the analysis of the EM properties of CVC and RVC foams, presenting various structures especially in terms of bulk densities and cells sizes. For that purpose, the evolution of the properties of those foams was analysed over the broadest frequency range ever investigated: from quasi-static (20 Hz) to microwave, terahertz and near-infrared frequencies.

2. Materials and methods

2.1 Materials

As explained in the introduction, the CVC foams investigated here were thoroughly described in a previous paper in terms of synthesis protocol, average cell size, bulk density and vitreous carbon texture [1]. All CVC foams were prepared by carbonisation at 900°C of phenolic-furanic rigid foams whose formulations, detailed in [1], were called STD, PEG, TRITON, PLURO, PMDI, T1, T2, T3P, T3DE, T4, TW, PPPT and SF. The bulk densities and the cell sizes of these new materials could be tuned by using various amounts of blowing agent in the formulation of the organic precursor foams. As a result, samples presenting either different cell sizes for a same average bulk density, or a same average cell size for different bulk densities, were successfully produced.

One formulation called RT, however, led to carbon foams whose porous structure is only based on struts, i.e., without cell walls (see again Fig. 2). Since the carbon source was again phenolic-furanic resin, and because this material was pyrolysed at the same temperature of 900°C as before, it is a reticulated vitreous carbon (RVC) foam. In addition, other RVC foams were also prepared from polyurethane foams used as templates, by hydrothermal impregnation of resorcinol-formaldehyde resin followed by carbonisation as described in [2]. The foams prepared from templates having 30 to 80 pores per inch were called TRF and had very similar bulk densities ranging from 0.029 to 0.035 g cm^{-3} but cells of average diameters ranging from 2070 to 738 µm, respectively. In the present study, RVC foams were also prepared with the same templates but impregnated with a resin derived from furfuryl alcohol in order to get smaller cell sizes. This technique was already used in [23] to impregnate compressed expanded graphite. These new foams having 30, 45, 60 or 80 pores per inch were called TAF and had very similar bulk densities ranging from 0.031 to 0.036 g cm^{-3} but average cells diameters of 1271, 795, 582, 489 µm, respectively (see Fig. 3).

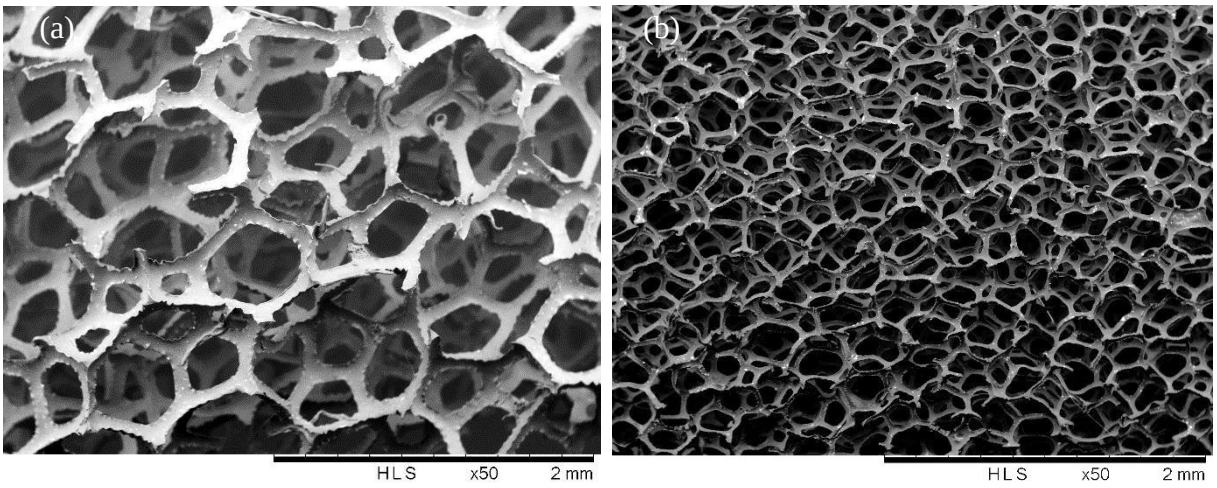

Fig. 3. Reticulated vitreous carbon foams (TAF formulation) derived from polyurethane templates having initially: (a) 30 pores per inch, and (b) 80 pores per inch.

Since most details about carbon foams structure were abundantly given and discussed in our former works [1,2,3], the reader is invited to refer to them. However, it is important to recall here some key data that are relevant to the present study and that will be required in Section 3. Such data, summarising sample name and corresponding average bulk density, overall porosity and average cell size, are gathered in Table 1.

Table 1. Main structural features of carbon foams analysed herein. The samples marked by a star are those having very different bulk densities but rather similar average cell sizes.

Foam's nature	Type of formulation	Bulk density (g cm^{-3})	Overall porosity (%)	Average cell size (µm)
CVC	PEG *	0.333	83.2	152
	PEG	0.187	90.6	293
	TRITON	0.158	92.0	296
	PLURO *	0.269	86.4	161
	PLURO *	0.140	92.9	212
	T2 *	0.129	93.5	112
	T2 *	0.088	95.6	186
	TW *	0.044	97.8	164
	T3P *	0.036	98.2	167
RVC	RT	0.047	97.6	779
	TRF	0.025	98.7	974
	TAF	0.031	98.4	489
	TAF	0.033	98.3	582
	TAF	0.036	98.2	795
	TAF	0.035	98.2	1271

2.2 Low-frequency measurements

The relative permittivity and the electrical conductivity were determined at low frequency, between 20 Hz and 1 MHz, with the Hewlett-Packard 4284A LCR-meter shown in Fig. S1 of the Electronic Supplementary Information. The method is based on the use of

equivalent electrical circuits. Selecting one of these allowed measuring capacitance C and loss tangent δ, from which the complex relative permittivity could be calculated by application of the plane capacitor formulae [24]:

$$\varepsilon' = \frac{(C_S - C_0)\,\tau}{\varepsilon_0\, A_S} + 1 \quad (1)$$

$$tg\,\delta = \frac{C_S\, tg\delta_S - C_0\, tg\delta_0}{C_S - C_0} \quad (2)$$

where C_S and tg δ_S are capacitance and loss tangent of the device with the sample under study, C_0 and tg δ_0 are the same for the sample-free device, τ and A_s are thickness and area of the sample, respectively, and ε_0 is the dielectric permittivity of vacuum. The electrical conductivity σ' was therefore calculated as:

$$\sigma' = \varepsilon' \text{ tg } \delta\, \varepsilon_0\, \omega \quad (3)$$

A second circuit of the LCR-meter, when selected, allowed determining the complex impedance $Z^* = X' + jX''$, where X' and X'' are real and imaginary parts of Z^*, respectively. The electrical conductivity thus reads:

$$\sigma = \frac{1}{X'}\frac{\tau}{A_S} \quad (4)$$

Whether calculated from Eq. (3) or (4), we checked that the values of the electrical conductivity were always similar within less than 1 %.

2.3 Microwave-frequency measurements

Carbon foams' properties in the microwave domain were investigated by using three different waveguide devices of rectangular cross-sections 23 × 10 mm², 7.2 × 3.4 mm² (see Fig. S2 of the Electronic Supplementary Information), and 2 × 4.3 mm² for measurements in X-band (8-12 GHz), Ka-band (26-38 GHz) and partially in V-band (40-53 GHz), respectively. An Elmika 2400 scalar network analyser was then used for determining the scalar scattering

parameters S_{21} (i.e., transmitted / input signal) and S_{11} (i.e., reflected / input signal). The power stabilisation was provided at the level of 7.0 mW ± 10 μW in the measurable EM attenuation range from 0 to 40 dB.

Rectangular samples in the shape of plates filling the cross-section of the waveguide allowed obtaining the coefficients of absorption, reflection and transmission: *A*, *R* and *T*, respectively. The complex dielectric permittivity was calculated according to the standard procedure described in [24]. Also, for the determination of dielectric properties, another more precise method was used [25]. According to the latter, rod-like samples such as the one shown in Fig. S2, having a diameter of about 1 mm, were used and placed at the centre of the waveguide with their axis parallel to the electric field vector. All samples were glued with silver paint to the sample holder. The dielectric properties of carbon foams investigated this way were then obtained by application of a modified Newton optimisation algorithm based on the waveguide formalism (see [24] for details).

2.4 IR and THz measurements

The electromagnetic properties of carbon foams were analysed at infrared frequencies by FT-IR spectroscopy in reflection and transmission using a Bruker Vertex 80v device working between 1.5 and 250 THz (i.e., corresponding to wavelengths in the range 1.2 – 200 μm), see Fig. S3(a) of the Electronic Supplementary Information. The range between microwave and infrared (IR) frequencies was studied with a time-domain THz spectrometer EKSLPA T-SPEC with a femtosecond laser (wavelength 1 μm, pulse duration less than 150 fs) and a photoconductive GaBiAs switch used as transmitter and detector from 100 GHz to 3 THz (quasi-optical method), see Fig. S3(b).

In order to investigate the mechanisms of transmission losses by absorption or reflection, experiments were carried out in reflection on eight different CVC foams using the Diffuse

Reflectance EasiDiff Pike accessory of the FT-IR spectrometer in the range 1.5 – 20 THz (see Fig. S3(c) of the Electronic Supplementary Information). During these tests, the incident radiation was reflected on the surface of the sample placed at the centre of a cavity. The latter is a reflection chamber generally used for powders and collecting all the signals reflected in various directions. It is noteworthy that this technique is not affected by the thickness of the sample, so that the samples already tested for transmission could be reused.

3. Results and discussion

3.1. Influence of bulk density

Carbon foams having very different densities, i.e., having different overall porosities, but rather similar average cell diameters (see the foams indicated by a star in Table 1) were analysed at low frequency (20 Hz – 1 MHz) and in the microwave range in the form of either small rods (for dielectric properties in the X-band) or plates (for coefficients *R*, *T* and *A* in the Ka-band).

3.1.1. Impact of bulk density on dielectric properties

The relative permittivity and the electrical conductivity of the carbon foams are shown in Fig. 4 as a function of bulk density. The permittivities and conductivities measured at 8.64 GHz increased from 12 to 70 and from 13 to 24 S m^{-1}, respectively, when the density increased from 0.036 to 0.333 g cm^{-3}. The conductivities were almost identical to those found at the same frequency for standard CVC foams described elsewhere [4], which indeed varied from 13 to 18 S m^{-1} for densities ranging from 0.048 to 0.114 g cm^{-3}.

In the static regime, the permittivity and the conductivity: $1 \times 10^5 < \varepsilon' < 6 \times 10^5$ and $4 < \sigma < 58$ S m^{-1}, respectively, were somewhat lower than the values reported earlier for standard CVC foams in [4].

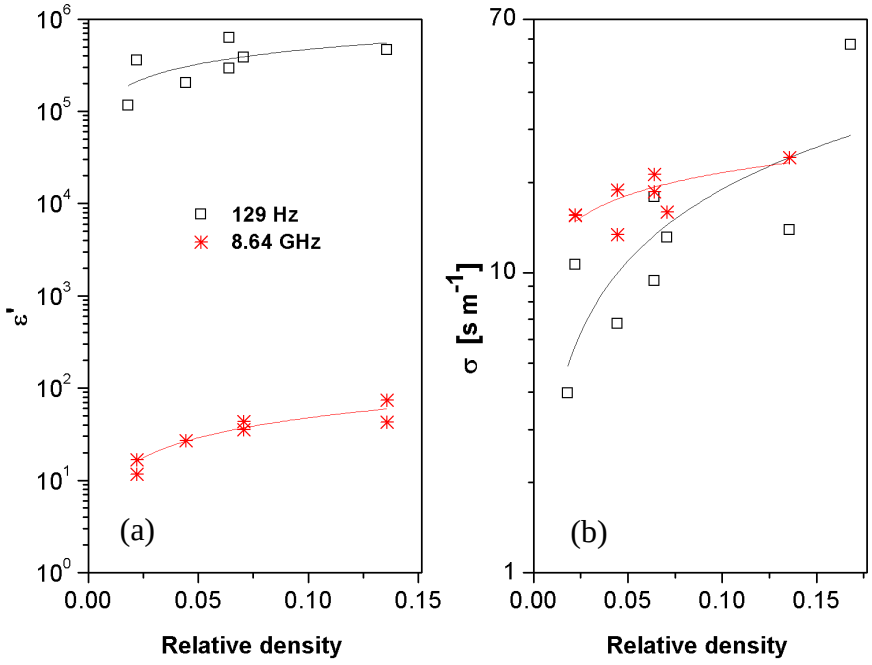

Fig. 4. (a) Dielectric permittivity and (b) electrical conductivity of the CVC foams marked with a star in Table 1, at different frequencies and as a function of relative density. The curves are fits of Eqs. (5) and (6) to the data of (a) and (b), respectively.

In a similar way to what was done in [4], power laws correctly fitted the results. The two corresponding exponents *t* and *s* were thus obtained by adjusting equations (5) and (6) to the experimental data found in the static regime and in the microwave domain (see Table 2):

$$\varepsilon' \sim (\rho / 1.98)^s \sim {d_r}^s \quad (5)$$

$$\sigma' \sim (\rho / 1.98)^t \sim {d_r}^t \quad (6)$$

where ρ (g cm^{-3}) is the bulk density of CVC foams, 1.98 (g cm^{-3}) is their skeletal density (see [1]), and d_r (dimensionless) is the relative density.

Table 2. Exponents *t* and *s* corresponding to the fits of equations (5) and (6) to the data of Fig. 4(a) and 4(b), respectively, and to the data of Fig. 6(a) and 6(b), respectively.

Carbon foams	Frequency	*t*	*s*
CVC foams with similar cell sizes but different densities	129 Hz	0.53	0.80
	8.64 GHz	0.72	0.25
CVC and RVC foams having various porous structures and densities	8.64 GHz	0.81	0.31
	26 GHz	0.73	0.41

Except for the parameter *t* at 129 Hz, the values determined here were similar to those previously found for standard CVC foams [4]. The lower value found for *t* can be explained by the adjustment carried out over a range of densities more than twice larger than before. Indeed, the materials with the highest density (0.333 g cm^{-3}) are closer to porous solids than to true foams, i.e., are not so close to the percolation threshold and thus might be out of the range of applicability of Eq. (6). The similarity of all other values with those reported for standard CVC foams seems to indicate that cell size has little or no influence on both conductivity and permittivity. However, further studies were carried out for confirming these observations and explaining the differences with the formerly published results (see next section 3.2). It should also be noticed that, due to the high porosity of these foams, to the possibly poor electrical contacts (especially at low frequency), and to the probable presence of impurities related to tannin used in the formulations, the electric conductivities are obviously much lower than the values reported for commercial, non-porous glass-like carbons pyrolysed at 900°C, around 7×10^3 S m^{-1} [26].

3.1.2. Impact of bulk density on A, R and T coefficients

Foams cut as parallelepipeds were analysed in the Ka-band (26 – 38 GHz) to observe the influence of density on the coefficients *A*, *R* and *T*. These parameters at 26 GHz are shown in

Fig. 5. It can be seen that the transmission is slightly higher than what was previously reported for standard CVC foams [4], whose values were found within the range 0.065 – 0.14 for 1.9 mm-thick samples. The electromagnetic shielding is here strongly dominated by reflection, with values significantly higher than those reported for standard CVC foams and increasing from 0.79 to 0.93 when the density increased from 0.036 to 0.333 g cm^{-3}. The absorption is then very low, and decreases from 0.1 to 0.01 within the same range of bulk density. All carbon foams having densities equal or higher than 0.14 g cm^{-3} present the same EM behaviour in this range of frequencies, showing almost zero absorption and very high reflection. This finding might be explained by the saturation of the curve of electrical conductivity at high bulk density (see again Fig. 4(b)).

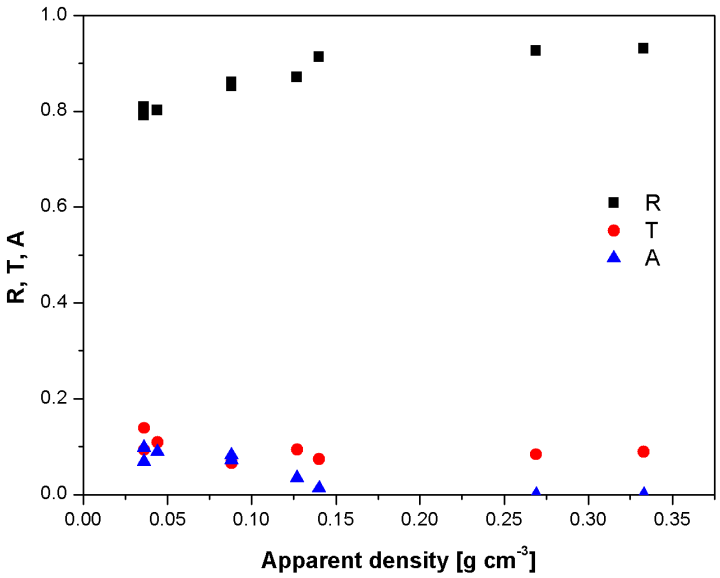

Fig. 5. Reflection, transmission and absorption coefficients at 26 GHz of 1.9 mm-thick CVC foams marked with a star in Table 1, as a function of bulk density.

Table 3 presents the parameter S_{11} and the electromagnetic shielding efficiency (*EMI SE*) of the same CVC foams as in Figs. 4 and 5. It can be observed that S_{11} is much higher than that of standard CVC foams (see [4]), whereas the *EMI SE* is slightly lower, with values from

9.44 to 11.81 dB for densities ranging from 0.036 to 0.333 g cm^{-3}, respectively. The *EMI SE* is maximal for densities 0.088 and 0.140 g cm^{-3}, corresponding to foams with the largest cell sizes, as shown in Table 1. However, such differences of cell size are not significant in order to conclude about a cell size effect, especially because no trend can be observed for the other foams.

Table 3. Parameter S_{11} (i.e., reflected / input signal) and electromagnetic interference shielding (*EMI SE*) determined at 26 GHz for 1.9 mm-thick CVC foams marked with a star in Table 1.

Bulk density (g cm^{-3})	S_{11} (dB)	*EMI SE* per 1.9 mm (dB)
0.333	- 0.31	10.51
0.269	- 0.33	10.76
0.140	- 0.40	11.31
0.129	- 0.60	10.27
0.088	- 0.67	11.81
0.044	- 0.96	9.63
0.036	- 0.97	9.44

Since such carbon foams have rather small cells and windows, it might be expected that it is more difficult for the EM radiations to penetrate into the materials, thus leading to a very strong reflection. However, the different *A*, *T* and *R* coefficients observed for these foams with respect to those of standard CVC foams reported in [4] are most probably due to differences in contact between the samples and the waveguides. This assumption is supported by the very similar values of complex relative permittivity presented by carbon foams in Fig. 4 in the microwave range. The importance of metal – carbon foam contact has already been addressed in a previous work [14], where it has been shown that a poor contact significantly reduces the measured electromagnetic shielding, and this effect increases with frequency. The

present foams have also small cells which make very difficult the removal of residues coming from the cutting of the sample. Small carbon debris blocked in the outermost porosity can thus locally increase the density and hence the reflection. The cell size has therefore probably a significant influence on the determination of EM parameters through differences of contact and surface quality. Those effects thus have nothing to do with the intrinsic properties of the materials under study, but rather arise from unavoidable experimental biases of the characterisation method.

Regarding the tests with rod-like samples, the contact area between the sample and the waveguide is located outside the zone under study, so the experimental biases due to possibly poor contacts are expected to be negligible. Transmission and reflection coefficients of thin plates inside waveguide were calculated from the dielectric data obtained according to the thin dielectric method [25], and very similar values to those presented in Fig. 5 (i.e., with an uncertainty less than 10%) were obtained. The dielectric properties and the EM shielding are linked with each other, and since it was observed above that the dielectric properties are independent of cell size, the same should apply for *A*, *R* and *T*. In other words, cells and windows sizes should have little or no influence on the electromagnetic shielding efficiency in the microwave frequency range.

3.2. Dielectric properties of carbon foams having different porous structures

Other carbon foams with various porous CVC and RVC structures have also been analysed in microwave frequencies at 8.64 and 26 GHz (see Fig. 6) in order to confirm the trends observed above. For more information regarding their structural properties, and as explained in the introduction, the reader should refer to [1].

Equations (5) and (6) were applied to the data of Fig. 6, and the corresponding exponents *t* and *s* are presented in Table 2. They are very similar to those found at 8.64 GHz, as well as

to the values determined for standard CVC foams at 26 GHz in [4]. It is important to stress that the carbon foams presented in Fig. 6 have a broad range of bulk densities (0.025 – 0.269 g cm^{-3}) but also of cells (165 – 974 μm) and windows sizes. Moreover, they belong to both CVC and RVC types. Despite this, and even if there is a non-negligible scattering of the results, finding very similar exponents *t* and *s* suggests again that the dielectric properties are dominated by the overall porosity (i.e., by the bulk density), and do not depend on cells or windows sizes. Also noteworthy is that there is no significant change in the values of *t* and *s* between 8.64 and 26 GHz. Herein, the effect of cells and windows size was investigated only at microwaves with the rod-like samples, because the effect of poor electrical contacts is negligibly small for such measurements in comparison with low-frequency data [4].

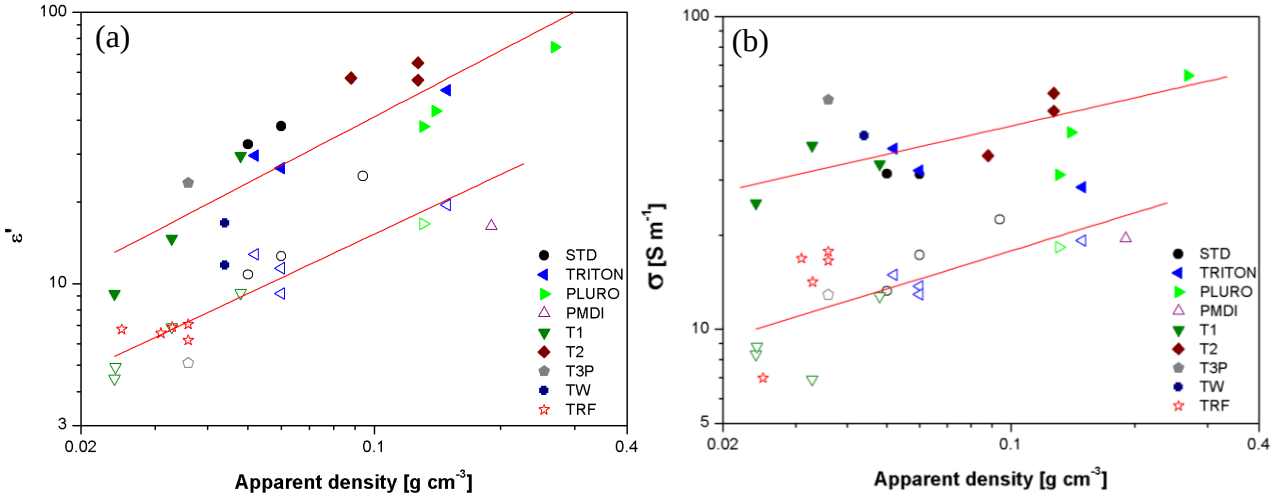

Fig. 6. (a) Dielectric permittivity and (b) electrical conductivity of different types of CVC and RVC foams, at 8.64 GHz (filled symbols) and at 26 GHz (open symbols), as a function of bulk density. The curves are fits of Eqs. (5) and (6) to the data of (a) and (b), respectively.

The absence of cell size effect is confirmed in Fig. 7, where CVC foams with similar bulk densities (0.048 g cm^{-3} < ρ < 0.060 g cm^{-3}) were analysed at 8.64 and 26 GHz. These data were compared with the dielectric properties of RVC foams (TRF formulation) at 26 GHz, and the latter materials did not show any trend related to cell size either.

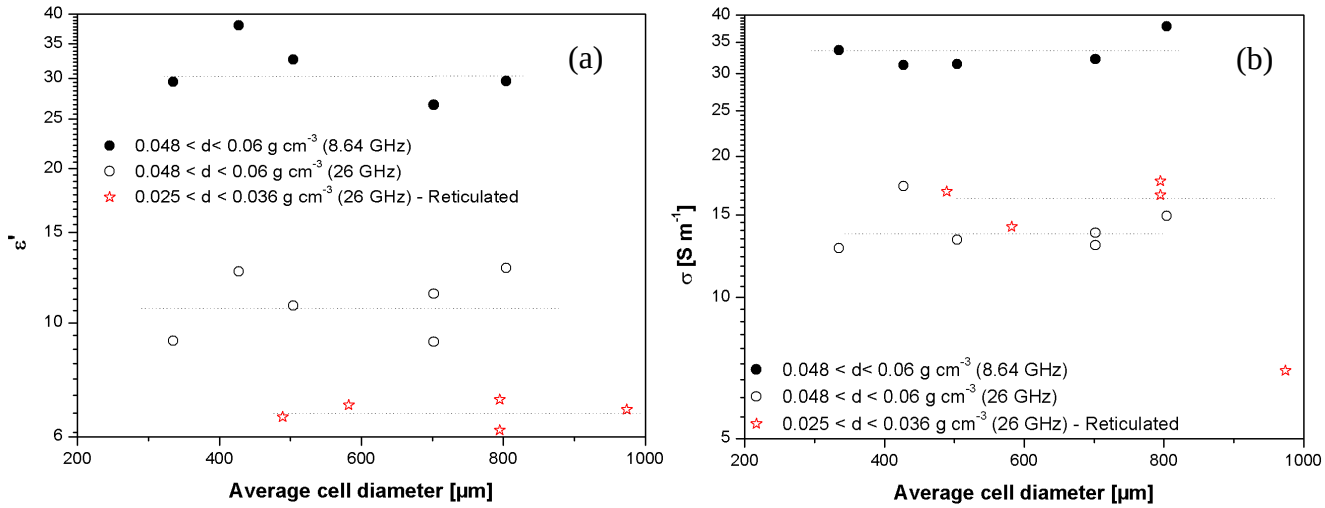

Fig. 7. (a) Dielectric permittivity and (b) electrical conductivity of CVC and RVC foams with similar densities at 8.64 GHz (filled symbols) and at 26 GHz (open symbols), as a function of average cell diameter. The red stars correspond to the TRF formulation of RVC foams, and the straight lines are just guides for the eye.

3.3. Dielectric properties as a function of frequency

Fig. 8 shows real (ε') and imaginary (ε'') parts of the permittivity of three carbon foams having different porous structures as a function of frequency in the microwave range (X-, Ka-, and V-bands). These are the foams of formulations TRITON, T3P and TRF with bulk densities of 0.059, 0.036 and 0.036 g cm^{-3}, respectively.

In all bands studied here it was found that ε' and ε'' decrease in different ways with frequency. The two foams of similar, low bulk densities (cellular and reticulated) exhibit the same behaviour, i.e., the imaginary part of the permittivity is higher than the real part up to a frequency of about 35 GHz, beyond which a crossover is observed. For the densest foam, however, the real part of the permittivity is higher than the imaginary part in the frequency range investigated here.

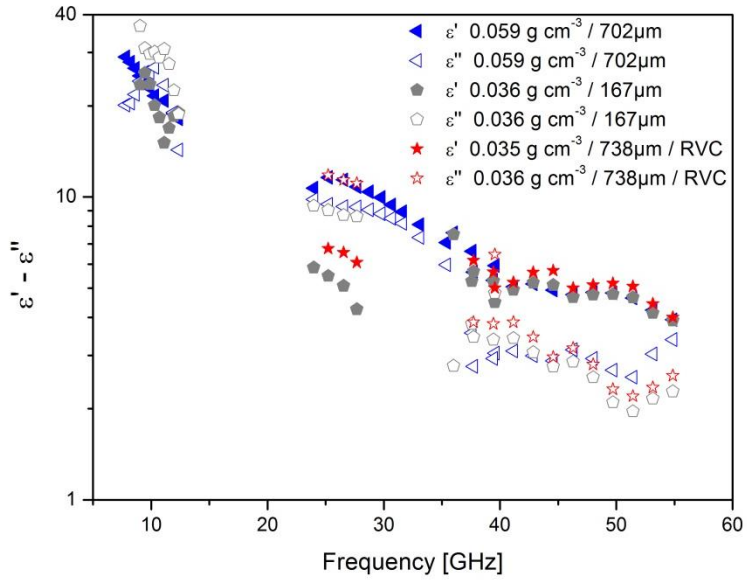

Fig. 8. Real (ε') and imaginary (ε'') parts of the permittivity of two CVC and one RVC foams as a function of frequency in the microwave range (X-, Ka- and U-bands). The RVC foam (red stars) is compared with one CVC foam of same density but different cell size, and with one CVC foam of same cell size but different density.

The values of permittivity of a few more carbon foams measured in the range 24 – 40 GHz (see Fig. S4 and S5 of the Electronic Supplementary Information) also confirm such a trend. Indeed, whatever the connectivity of the carbon foams (i.e., whether they are cellular or reticulated), and whatever the cell size, it was found in this frequency range that ε'' is higher than ε' for materials whose density is lower than about 0.036 g cm^{-3}. The permittivities of the foams of higher density exhibit the opposite tendency in the same frequency range (see Fig. S4 of the Electronic Supplementary Information).

Such a change of EM behaviour as a function of foam density can be observed more clearly by comparing the loss tangents (tg $\delta = \varepsilon'' / \varepsilon'$) at two different microwave frequencies of 8.64 and 26 GHz as shown in Fig. 9. In the latter, the different types of carbon foams were not distinguished since it was found above that the porous structure has no effect on

permittivity at constant porosity. Despite some natural scattering of the data, the loss tangent clearly decreases when the density increases, and becomes lower than 1 above 0.047 g cm^{-3} for both frequencies 8.64 and 26 GHz.

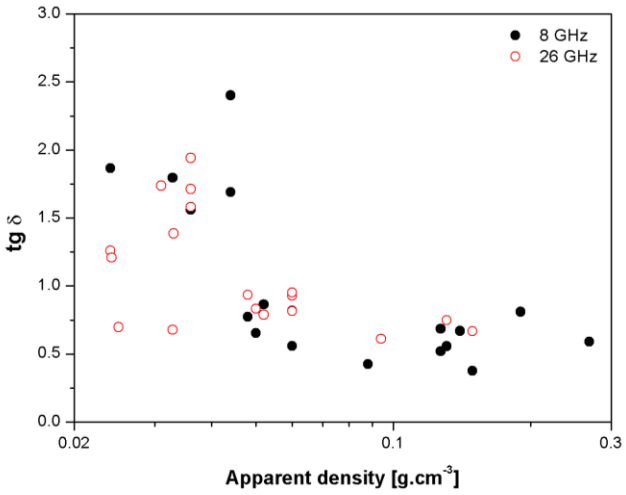

Fig. 9. Loss tangent (tg $\delta = \varepsilon'' / \varepsilon'$) as a function of bulk density of the same carbon foams as in Fig. 6, at 8.64 and 26 GHz.

This observation can be easily explained by the study of the influence of bulk density on the dielectric properties which was carried out above. It was indeed shown that ε', σ and therefore ε'' ($\varepsilon'' = \sigma / \varepsilon_0 \omega$) increase with the density according to power laws of exponents t and s, respectively. It was found that ε' increases faster with density than ε'' in microwaves (see Table 2); this is consistent with Fig. 9 since tg δ decreases with density. Moreover, both ε' and σ change with density according to power laws, so their variations at high density are moderate, which is also the case for tg δ. This decrease of tg δ with density is a noticeable phenomenon when compared, for example, with what happens for metals, showing large loss tangents, or for composites whose tg δ increases with the concentration of conductive filler [27]. It is likely that the conductivity and therefore the tangential losses both become very important when the density increases until it approaches that of non-porous vitreous carbon.

In order to explain the variation of these tangential losses with frequency, it is interesting to consider the complex impedance Z^* of carbon foams. This method was already considered in [6] but only a few foams were analysed at that time. It reads:

$$Z^* = 1/(\,j\,\varepsilon_0\,\omega\,\varepsilon) = Z' - j\,Z'' \tag{7}$$

$$Z' = \varepsilon'' / [\varepsilon_0 \omega\,(\varepsilon'^2 + \varepsilon''^2)] \tag{8}$$

$$Z'' = \varepsilon' / [\varepsilon_0 \omega\,(\varepsilon'^2 + \varepsilon''^2)] \tag{9}$$

It has been observed that ε' and ε'' both decrease with frequency and therefore, according to equations (8) and (9), $Z' = Z''$ when $\varepsilon' = \varepsilon''$. The variation of impedance can also be explained through an analogy with a simple RC circuit such as:

$$Z^* = X' / (1 + j\,X'C\omega) \tag{10}$$

$$Z' = X' / (1 + (X'C\omega)^2) \tag{11}$$

$$Z'' = X'^2 C\omega / (1 + (X'C\omega)^2) \tag{12}$$

According to equations (11) and (12), $Z' = Z''$ (and thus $\varepsilon' = \varepsilon''$) at the angular frequency $\omega_0 = 1/X'C$. The electrical resistance X' of the carbon foams is proportional to the inverse of the DC conductivity according to the relation (4), and is therefore proportional to the inverse of ε'' at frequencies below 1 MHz (i.e., where electrical conductivity coincides with DC conductivity). The capacitance C is directly linked to ε' at low frequency through Eq. (1). Thus, the angular frequency ω_0 is proportional to tg δ and thus decreases with the density of the foams. The curves of ε' and ε'' intersect at the frequency ω_0 and the behaviour of carbon foams therefore change from more resistive to more capacitive with lower losses. However, it should be noticed that Z'' is maximum at a slightly higher frequency ω_m such that $\omega_m = 1/\sqrt{X'C}$. Thus, between ω_0 and ω_m, the loss tangent still decreases significantly. Beyond ω_m, the two parts of the permittivity decrease slowly and tg δ therefore becomes rather constant.

To conclude, at low frequency, the carbon foam impedance is high and characterised by high losses (see for instance the strong decrease of tg δ at low frequencies in [9]). The properties of carbon foams over the whole range of radiofrequencies can be nevertheless controlled through their bulk density. When the latter increases, the conductivity and the real part of the permittivity increase, which then lead to an increase of reflection (see [9]). As the density increases, the behaviour of the foams therefore gets closer to that of a metal with high reflectivity and low absorption.

The impedance of carbon foams increases with frequency up to a maximum corresponding to $\varepsilon' = \varepsilon''$ or $\omega_0 = 1/X'C$, which seems to appear in the microwave range (at about 35 GHz for foams of density $\rho \approx 0.035$ g cm^{-3}). The frequency at which the imaginary part of the complex impedance is maximum is proportional to tg δ at low frequencies (below 1 MHz), and therefore decreases with density. In conclusion, the behaviour of carbon foams changes from that of a metal with high impedance, high reflection and low absorption at low frequency, to that of a conductor with losses at the frequency ω_0. Above ω_m, impedance and tangential losses decrease slowly, and carbon foams progressively turn from more resistive to more capacitive; they become less reflective and absorption becomes the main mechanism of EMI shielding.

3.4. EM behaviour in THz-IR ranges

3.4.1 Tests in transmission

Carbon foams were investigated in three different frequency ranges, 0.1-3 THz (by Terahertz Time-domain spectroscopy), 1.5-20 THz and 12-250 THz (by FT-IR spectroscopy), so as to obtain an overall view of the changes of properties with frequency. The thickness of all samples at these frequencies was approximately 1.2 mm. It had been found above that transmission in the microwave domain is low for all foams, whether they are reticulated or

cellular. For frequencies higher than 0.1 THz, however, a clear difference can be seen between cellular and reticulated foams (see Fig. 10).

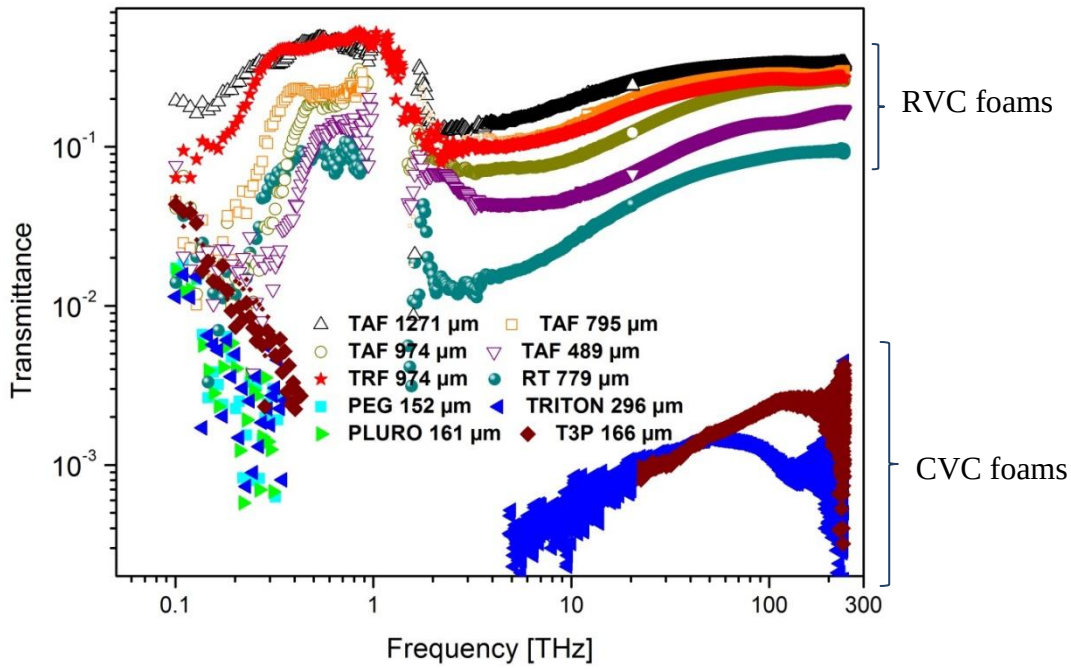

Fig. 10. Transmittance of carbon foams measured in IR and THz ranges. The average cell diameter is indicated in the legend.

For CVC foams, the transmission tends to decrease, from about 0.01 - 0.05 to values as low as 10^{-3}, when the frequency increases from 0.1 to 1 THz. These foams transmit almost no signal (even at the lowest possible thickness, about 100 µm); the data are highly scattered and sometimes poorly exploitable. Indeed, CVC foams are opaque in the THz-IR range. Regarding RVC foams, the transmission is not negligible and increases with frequency in both THz and IR domains. Looking at the transmission curves of TAF foams having increasing cell size (from 489 µm to 1271 µm), it is noteworthy that transmission increases with cell (or window) size. The reticulated foam derived from tannin, RT, has a low transmission which can be attributed to its higher bulk density but most probably to the higher heterogeneity of this foam.

Broad transmission peaks between about 0.2 and 3 THz can be conjectured from the data of Fig. 10 for all RVC foams, but are not easily observed as they fall between two ranges of investigated frequencies. The absorbance was calculated according to the Beer-Lambert law and is given as a function of wavenumber in Fig. 11 for enabling the comparison with data from the literature, generally presented this way in the IR range. In the investigated domain, the transmission significantly depends on cell size. The three following features may be observed: (i) a global increase of transmission with frequency, on average, for all RVC foams above 1 THz, the increase being faster for lower cell sizes; (ii) the transmission peak becomes broader and more intense when the cell size increases; and (iii) the frequency at which the transmission stabilises ranges from a few tens to a few hundreds of THz and increases when the cell size decreases. The latter two characteristics (ii) and (iii) are probably related to a resonance phenomenon corresponding to the transmission peak that appears at around 1 THz.

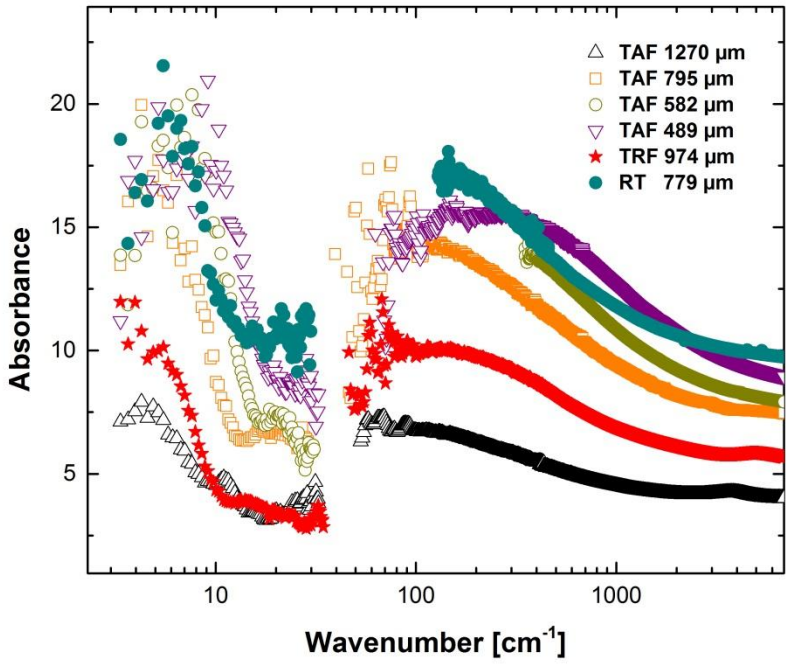

Fig. 11. Absorbance of RVC foams in THz and IR frequency ranges. The average cell diameter and types of formulation are indicated in the legend.

The study of this frequency domain is still rather uncommon. Carbonaceous materials are indeed generally characterised by Raman spectroscopy and most of the time present at least two main characteristic peaks corresponding to phonon resonances that should be located at the end of the range investigated here, i.e., close to 18100 and 17900 cm^{-1} for an excitation at 514 nm (i.e., an incident energy of 2.41 eV). On the other hand, infrared spectrometry studies usually deal with wavenumbers above 500 cm^{-1} [28–30]. Coals derived from the carbonisation of biomass were investigated in terahertz spectroscopy between 250 and 500 cm^{-1} [31]. However, and as far as we know, the transmission peak around 1 THz observed here has never been reported in the literature for carbon materials.

Since such transmission peak in the THz range depends on the structure of the foam, one might think of a waveguide-like effect. The cells or the windows might indeed be seen as many waveguides throughout which only certain types of monochromatic waves, called modes, could propagate depending on the dimensions of those waveguides. If the latter are assumed to behave like rectangular waveguides, they may act as high-pass filters where different modes having different cut-off frequencies can be propagated. The mode corresponding to the lowest cut-off frequency is the fundamental mode (TE_{10} for a rectangular waveguide).

Considering cells or windows as rectangular waveguides and looking only at the fundamental mode, the cut-off frequency, f_c, and the frequency corresponding to the maximum transmission, f_m, can be calculated using the average windows or cells diameters from the following equations:

$$f_c = c / 2a \quad (13)$$

$$f_m = 2c / a \quad (14)$$

where *a* is either cell or window size, and *c* is the speed of light. The frequencies corresponding to the minimum and maximum transmissions in the THz range were measured from the data of Fig. 10 and then compared with the values calculated from Eqs. (13)-(14) by considering either cells or windows as waveguides. The results are given in Fig. 12(a)) and 12(b), respectively.

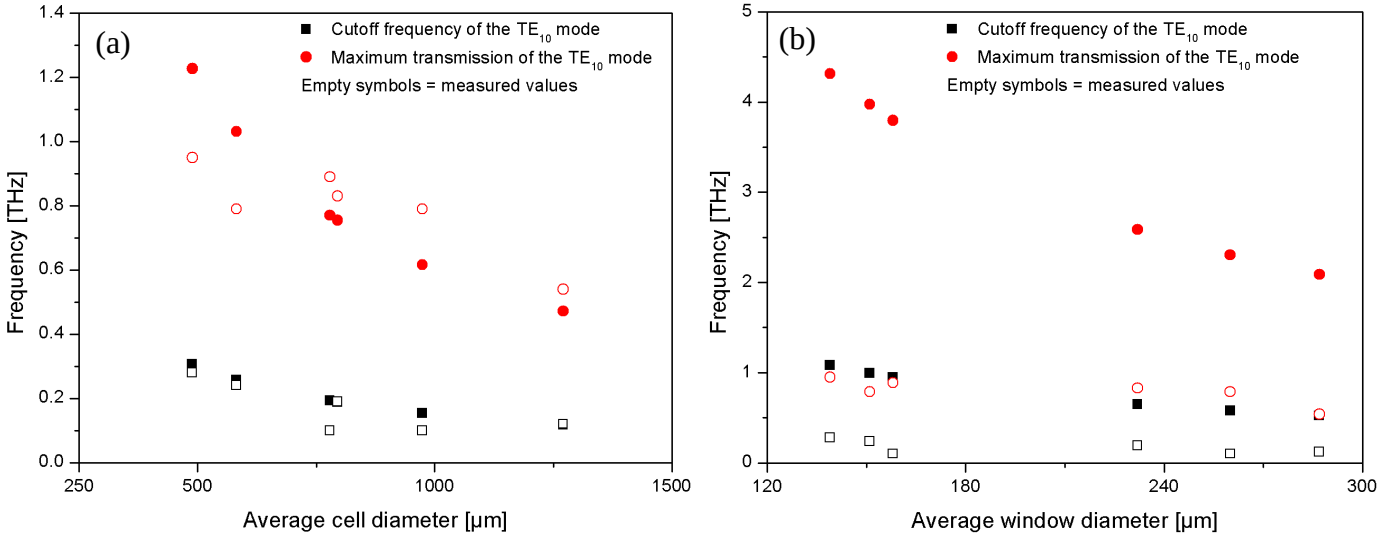

Fig. 12. Comparison of calculated cut-off and maximum transmission frequencies of the TE_{10} mode by considering: (a) cells, and (b) windows of RVC foams as rectangular waveguides.

It is then easy to see that the values calculated by considering cells as waveguides (Fig. 12(a)) are in good agreement with the experimental data, whereas the frequencies calculated based on window sizes (Fig. 12(b)) are significantly higher than the measured values. Such simple relationships between EM properties of foams and those of rectangular waveguides allow defining the frequency at which transmission begins to increase and that at which it is the highest. As mentioned above, waveguides behave as high-pass filters where different modes can propagate. Now, for RVC foams, the maximum of transmission is followed by a fast and significant drop, and a maximum transmission is only found around a few hundred

THz. It is then possible that higher order modes are strongly damped and therefore difficult to observe on the transmission curves.

Another possible explanation of such peak followed by a decrease of transmission is related to the excitation of surface plasmons, which is a well-known phenomenon in the THz frequency range for multiply-perforated metal plates [32–38]. These plasmons correspond to the collective oscillations of electrons of a conductor material at the interface with a dielectric medium (here air). Those surface waves can then go into resonance under the action of electromagnetic radiations. In the particular case of conductive plates perforated with multiple holes, periodically or not, very intense transmission peaks arising from particular modes of plasmons resonance are observed. Higher transmissions than expected through the holes are then observed due to these particular resonances. This kind of phenomenon is interesting here because it depends on the size of the perforations and appears in the form of transmission peaks of tailorable width, depending on the porous structure. The characteristic wavelength λ of these plasmons, corresponding to the minimum of transmission after the peak, is expressed as a function of the size of the perforations a (here cell or window size) and of the dielectric permittivity of the material ε_m (here, of the struts) according to [36]:

$$\lambda = \frac{a\sqrt{\varepsilon_m}}{\sqrt{(m^2+n^2)}} \qquad (15)$$

where m and n correspond to the different orders of resonance of the surface plasmons. Further studies are needed to determine the dielectric permittivity of the struts and calculate this wavelength. However, if we consider a dielectric constant of 3 (i.e., a value intermediate between those of hexagonal graphite measured along (3.8) and perpendicular (2.61) to the carbon layers [39]) and assuming that $m = n = 1$, one finds frequency values in the range 0.2 – 0.5 THz for cell sizes of 1000 and 500 µm, respectively. These values are not far from the cutoff frequencies observed in Fig. 12(a), about 0.15 and 0.25 THz for cell sizes of 1000 and

500 µm, respectively. The absence of other transmission peaks and the gradual increase of transmission at higher frequencies may be due to the absence of higher order surface plasmons. These very complex notions will not be further detailed here and deserve additional research.

3.4.2 Tests in reflection

CVC foams exhibit very low reflection in the THz range, which decrease with frequency typically above about 1.5 THz (see Fig. 13). It is also noticeable that reflection peaks are observed at frequencies similar to those observed for transmission (see again Fig. 10). Reflection increases slightly with density. The two densest foams indeed present the highest reflections up to 20 THz. However, the very small carbon fragments produced when cutting such dense foams are very difficult to extract and may obstruct the outermost cells, thus increasing the reflection. It can be observed here that the reflection, which was preponderant in the microwave domain, decreases with frequency and becomes negligible in the THz range. Since these foams also have almost zero transmission, it can be concluded that CVC foams majorly absorb THz and IR radiations.

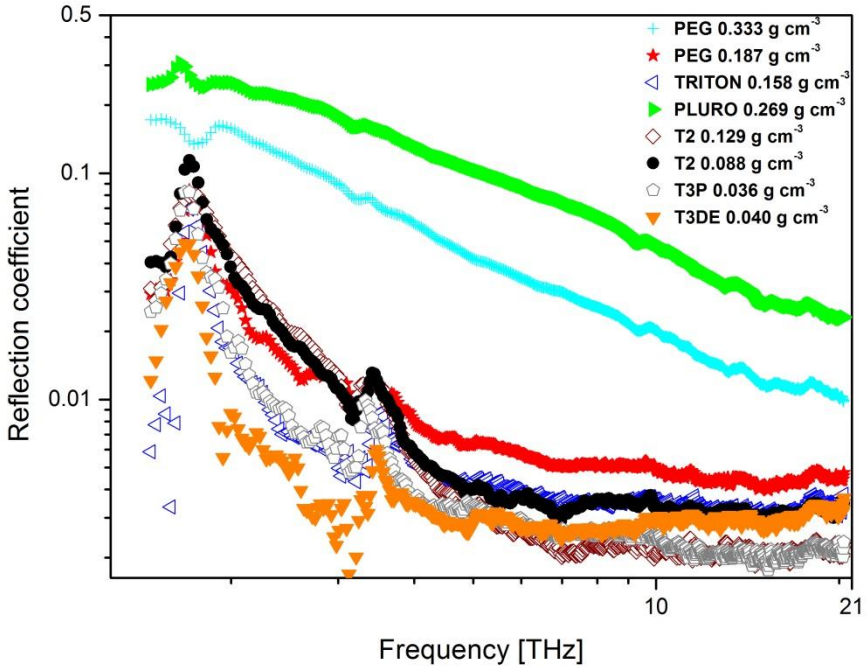

Fig. 13. Reflection coefficient of CVC foams, whose bulk densities are given in the legend, between 1.5 and 20 THz.

These results are consistent with a previous paper [40] dealing with the radiative properties of standard CVC foams in mid and far-infrared ranges: 24 to 214 THz (i.e., corresponding to the range of wavelengths 1.4 – 12.5 μm). In this former work, it was shown that tannin-based carbon foams have very high absorbances and low thermal conductivities that depend very little on frequency. It was also shown there that their total emissivity and the radiative part of their thermal conductivity increase with temperature. CVC foams therefore have behaviour close to that of black bodies in the THz and IR range.

4. Conclusion

The influence of the structure of carbon foams on their electromagnetic properties was investigated over a very broad frequency range: from quasi-static and low-frequency regime (20 Hz to 1 MHz), to microwave (in 3 frequency ranges 8-12, 24-40 and 35-55 GHz), terahertz (100 GHz to 3 THz), and finally near-infrared (1.5-250 THz) domains.

It was found that bulk density is the parameter controlling the EM properties up to around 50 GHz, i.e., for wavelengths much higher than the main geometric parameters of foams. Just like in a percolating system, the real part of the permittivity and the conductivity increase with density according to power laws whose exponents decrease with frequency. It is noticeable that the real part of the permittivity increases faster with density than the conductivity. However, no change of the EM properties was found by varying other structural parameters such as cell size or interconnectivity, the latter parameter being related to the CVC or RVC nature of foams.

At low frequency, the imaginary part of the permittivity is higher than the real part. Thus, the foams behave as metals with high impedance and high losses. When the density increases, both the electrical conductivity and the real part of the permittivity increase. As a consequence, reflection of EM waves increases and absorption decreases. The imaginary part drops faster than the real part when the frequency increases, and therefore both converge towards the same value. The frequency at which $\varepsilon' = \varepsilon''$ decreases with density. It was observed that for carbon foams of density 0.036 g cm^{-3}, this frequency is around 35 GHz, and it may be conjectured for foams of higher density that it should range from 1 MHz to 8 GHz (a domain not studied here). At the frequency such that $\varepsilon' = \varepsilon''$, carbon foams behave as lossy conductors. It was thus indeed found that the reflection of EM waves decreases with frequency whereas the absorption increases. Above the frequency such that $\varepsilon' = \varepsilon''$, the foams become more capacitive than resistive, the impedance and the loss tangent decrease slowly, and the absorption becomes the main mechanism.

The study of the electromagnetic properties in THz and IR ranges confirmed that the behaviour of carbon foams changes at the end of the microwave domain, i.e., above around 50 GHz. For CVC foams, transmission and reflection decrease and tend to be negligible in the IR domain. Carbon foams thus behave like black bodies which transform all the radiations into heat. However, RVC foams exhibit transmissions that are not negligible and that increase with cell size. The density does not appear having any significant influence in the THz-IR range, whether for RVC or CVC foams.

Resonance phenomena are observed for RVC foams between about 0.2 and 3 THz. At these frequencies, the wavelength is indeed of the same order of magnitude as the cell size. It was shown that the frequencies corresponding to the minima and maxima of transmission of these resonance peaks can be determined by considering the fundamental mode TE_{10} of a

rectangular waveguide whose larger dimension is the average cell diameter. The decrease in transmission observed at a frequency of a few THz is, however, not clearly explained. This phenomenon may be related to surface plasmon excitation, but further studies would be required for describing accurately such phenomenon. Better understanding the latter might allow using RVC foams as cheap and easily produced band-pass filters, whose cut-off frequencies might be controlled through their cell size.

Acknowledgements

The authors gratefully acknowledge the financial support of the CPER 2007-2013 "Structuration du Pôle de Compétitivité Fibres Grand'Est" (Competitiveness Fibre Cluster), through local (Conseil Général des Vosges), regional (Région Lorraine), national (DRRT and FNADT) and European (FEDER) funds, as well as that of the project FP7-610875 NAMICEMC, Call ID FP7-PEOPLE-2013-IRSES. The authors also thank the support of the Institut Universitaire de France, by which this project could be carried out, as well as the "Gilibert" PHC exchange project "Dielectric and electric properties of hollow carbon spheres and mesoporous carbon" between France and Lithuania. PK is thankful for support by Tomsk State University Competitiveness Improvement Program.

References

[1] Letellier M, Szczurek A, Basso MC, Pizzi A, Fierro V, Ferry O, et al. Preparation and structural characterisation of model cellular vitreous carbon foams. Carbon 2017; 112: 208-18.

[2] Letellier M, Delgado-Sanchez C, Khelifa M, Fierro V, Celzard A. Mechanical properties of model vitreous carbon foams. Carbon 2017; 116: 562-71.

[3] Letellier M, Ghaffari Mosanenzadeh S, Naguib H, Fierro V, Celzard A. Acoustic properties of model cellular vitreous carbon foams. Carbon 2017; 119:241-50.

[4] Letellier M, Macutkevic J, Paddubskaya A, *et al.* Tannin-Based Carbon Foams for Electromagnetic Applications. *IEEE Trans. Electromagn. Compat.* , 1–7 (2015).

[5] Kuzhir PP, Paddubskaya AG, Shuba MV, Maksimenko SA, Celzard A, Fierro V, et al. Electromagnetic shielding efficiency in Ka-band: carbon foam versus epoxy/carbon nanotube composites. J Nanophotonics 2012; 6(1):61715.

[6] Letellier M, Macutkevic J, Paddubskaya A, Klochkov A, Kuzhir P, Banys J, et al. Microwave Dielectric Properties of Tannin-Based Carbon Foams. Ferroelectrics 2015; 479(1):119–26.

[7] Bychanok D, Plyushch A, Piasotski K, Paddubskaya A, Voronovich S, Kuzhir P, et al. Electromagnetic properties of polyurethane template-based carbon foams in Ka-band. Phys Scr. 2015;90(9): 094019-1 – 6.

[8] Bychanok D, Plyushch A, Kuzhir P, Macutkevic J, Letellier M, Szczurek A, et al. Tannin-based carbon foams in microwave frequency range: Toward fully carbon photonic crystal. Extended abstracts, IEEE 2015 International Conference on Microwaves,

Communications, Antennas and Electronic Systems (COMCAS). Tel Aviv (Israel) : 2015 : p. 1–3.

[9] Kuzhir PP, Paddubskaya AG, Maksimenko SA, Celzard A, Fierro V, Amaral-Labat G, et al. Highly porous conducting carbon foams for electromagnetic applications. International Symposium on Electromagnetic Compatibility 2012 (EMC EUROPE). Rome(Italy) : 2012 : p. 1–4.

[10] Yang J, Shen Z, Hao Z. Microwave characteristics of sandwich composites with mesophase pitch carbon foams as core. Carbon 2004; 42(8–9):1882–5.

[11] Fang Z, Cao X, Li C, Zhang H, Zhang J, Zhang H. Investigation of carbon foams as microwave absorber: Numerical prediction and experimental validation. Carbon 2006; 44(15):3368–70.

[12] Fang Z, Li C, Sun J, Zhang H, Zhang J. The electromagnetic characteristics of carbon foams. Carbon. 2007; 45(15):2873–9.

[13] Moglie F, Micheli D, Laurenzi S, Marchetti M, Mariani Primiani V. Electromagnetic shielding performance of carbon foams. Carbon 2012; 50(5):1972–80.

[14] Micheli D, Morles RB, Marchetti M, Moglie F, Mariani Primiani V. Broadband electromagnetic characterization of carbon foam to metal contact. Carbon 2014; 68:149–58.

[15] Micheli D. Mitigation of Human Exposure to Electromagnetic Fields Using Carbon Foam and Carbon Nanotubes. Engineering 2012; 4(12):928–43.

[16] Albano M, Micheli D, Gradoni G, Morles RB, Marchetti M, Moglie F, et al. Electromagnetic shielding of thermal protection system for hypersonic vehicles. Acta Astronaut 2013 ; 87:30–9.

[17] Zhang Y, Huang Y, Zhang T, Chang H, Xiao P, Chen H, et al. Broadband and Tunable High-Performance Microwave Absorption of an Ultralight and Highly Compressible Graphene Foam. Adv Mater 2015; 27(12):2049–53.

[18] Chen Z, Xu C, Ma C, Ren W, Cheng H-M. Lightweight and Flexible Graphene Foam Composites for High-Performance Electromagnetic Interference Shielding. Adv Mater 2013; 25(9):1296–300.

[19] Zhao W, Pizzi A, Fierro V, Du G, Celzard A. Effect of composition and processing parameters on the characteristics of tannin-based rigid foams. Part I: Cell structure. Mater Chem Phys. 2010; 122(1):175–82.

[20] Amaral-Labat G, Gourdon E, Fierro V, Pizzi A, Celzard A. Acoustic properties of cellular vitreous carbon foams. Carbon 2013; 58:76–86.

[21] Zhao W, Fierro V, Pizzi A, Du G, Celzard A. Effect of composition and processing parameters on the characteristics of tannin-based rigid foams. Part II: Physical properties. Mater Chem Phys 2010; 123(1):210–7.

[22] Kumar P, Topin F, Vicente J. Determination of effective thermal conductivity from geometrical properties: Application to open cell foams. Int J Therm Sci 2014; 81:13–28.

[23] Celzard A, Kresiñska M, Bégin D, Marêché JF, Puricelli S, Furdin G. Preparation, electrical and elastic properties of new anisotropic expanded graphite-based composites. Carbon 2002; 40: 557-66.

[24] Grigas J. Microwave Dielectric Spectroscopy of Ferroelectric and Related Materials. Gordon and Breach Science Publishing ; 1996.

[25] Standard Test Method for Measuring Relative Complex Permittivity and Relative Magnetic Permeability of Solid Materials at Microwave Frequencies, ASTM D5568-08, 2008, 2012.

[26] Soukup L, Gregora I, Jastrabik L, Konakova A. Raman spectra and electrical conductivity of glassy carbon. Mater Sci Eng B 1992; 11: 355–7.

[27] Saini P, Choudhary V, Singh BP, Mathur RB, Dhawan SK. Polyaniline–MWCNT nanocomposites for microwave absorption and EMI shielding. Mater Chem Phys 2009; 113(2–3):919–26.

[28] Dovbeshko GI, Romanyuk VR, Pidgirnyi DV, Cherepanov VV, Andreev EO, Levin VM, et al. Optical Properties of Pyrolytic Carbon Films Versus Graphite and Graphene. Nanoscale Res Lett 2015; 10(1) 234-1-6.

[29] Wang H, Guo JQ, Zhou YS. Understanding terahertz optical properties of amorphous carbon thin films. Carbon 2013; 64:67–71.

[30] Kaufman JH, Metin S, Saperstein DD. Symmetry breaking in nitrogen-doped amorphous carbon: Infrared observation of the Raman-active G and D bands. Phys Rev B 1989; 39(18):13053.

[31] Lepodise LM, Horvat J, Lewis RA. Signature of aromatic carbons in the terahertz spectroscopy of bio-chars. Extended abstracts, 38th International Conference on Infrared, Millimeter, and Terahertz Waves (IRMMW-THz) IEEE. Mainz(Germany) : 2013 : p. 1–2.

[32] Nguyen TD, Liu S, Kumar G, Nahata A, Vardeny ZV. Terahertz plasmonic properties of highly oriented pyrolytic graphite. Appl Phys Lett 2013; 102(17):171107.

[33] Lee J, Seo M, Kang D, Khim K, Jeoung S, Kim D. Terahertz Electromagnetic Wave Transmission through Random Arrays of Single Rectangular Holes and Slits in Thin Metallic Sheets. Phys Rev Lett 2007; 99(13): 137401-1-4.

[34] Vincenti MA, de Ceglia D, Grande M, D'Orazio A, Scalora M. Tailoring Absorption in Metal Gratings with Resonant Ultrathin Bridges. Plasmonics 2013; 8(3):1445–56.

[35] Garcia-Vidal FJ, Martin-Moreno L, Ebbesen TW, Kuipers L. Light passing through subwavelength apertures. Rev Mod Phys 2010; 82(1):729–87.

[36] Yang Y, Grischkowsky DR. High-Resolution THz Transmission and Reflection Measurements and Consequent Understanding of Resonant Hole-Arrays. IEEE Trans Terahertz Sci Technol 2013; 3(2):151–7.

[37] He X, Lu H. Graphene-supported tunable extraordinary transmission. Nanotechnology 2014; 25(32):325201.

[38] Gómez Rivas J, Schotsch C, Haring Bolivar P, Kurz H. Enhanced transmission of THz radiation through subwavelength holes. Phys Rev B 2003; 68(20): 201306-1-4.

[39] Delhaes P. Carbon Based Solids and Materials. Wiley-ISTE ; 2015.

[40] Celzard A, Tondi G, Lacroix D, Jeandel G, Monod B, Fierro V, et al. Radiative properties of tannin-based, glasslike, carbon foams. Carbon 2012; 50(11):4102–13.

Caption of Tables

Table 1: Main structural features of carbon foams analysed herein. The samples marked by a star are those having very different bulk densities but rather similar average cell size.

Table 2: Exponents *t* and *s* corresponding to the fits of equations (5) and (6) to the data of Fig. 4(a) and 4(b), respectively, and to the data of Fig. 6(a) and 6(b), respectively.

Table 3: Parameter S_{11} (i.e., reflected / input signal) and electromagnetic interference shielding (*EMI SE*) determined at 26 GHz for 1.9 mm-thick CVC foams marked with a star in Table 1.

Caption of Figures

Figure 1: Schematic structure of a reticulated carbon foam, emphasising the difference between cells and windows (i.e., holes connecting the cells).

Figure 2: Typical SEM pictures of: (a) CVC foam (formulation PPPT; density 0.094 g cm^{-3}), and (b) RVC foam (formulation RT, density 0.043 g cm^{-3}).

Figure 3: Reticulated vitreous carbon foams (TAF formulation) derived from polyurethane templates having initially: (a) 30 pores per inch, and (b) 80 pores per inch.

Figure 4: (a) Dielectric permittivity and (b) electrical conductivity of the CVC foams marked with a star in Table 1, at different frequencies and as a function of relative density. The curves are fits of Eqs. (5) and (6) to the data of (a) and (b), respectively.

Figure 5: Reflection, transmission and absorption coefficients at 26 GHz of 1.9 mm-thick CVC foams marked with a star in Table 1, as a function of bulk density.

Figure 6: (a) Dielectric permittivity and (b) electrical conductivity of different types of CVC and RVC foams, at 8.64 GHz (filled symbols) and at 26 GHz (open symbols), as a function of bulk density. The curves are fits of Eqs. (5) and (6) to the data of (a) and (b), respectively.

Figure 7: (a) Dielectric permittivity and (b) electrical conductivity of CVC and RVC foams with similar densities at 8.64 GHz (filled symbols) and at 26 GHz (open symbols), as a function of average cell diameter. The red stars correspond to the TRF formulation of RVC foams, and the straight lines are just guides for the eye.

Figure 8: Real (ε') and imaginary (ε'') parts of the permittivity of two CVC and one RVC foams as a function of frequency in the microwave range (X-, Ka- and U-bands).

The RVC foam (red stars) is compared with one CVC foam of same density but different cell size, and with one CVC foam of same cell size but different density.

Figure 9: Loss tangent (tg $\delta = \varepsilon'' / \varepsilon'$) as a function of bulk density of the same carbon foams as in Fig. 6, at 8.64 and 26 GHz.

Figure 10: Transmittance of carbon foams measured in IR and THz ranges. The average cell diameter is indicated in the legend.

Figure 11: Absorbance of RVC foams in THz and IR frequency ranges. The average cell diameter and types of formulation are indicated in the legend.

Figure 12: Comparison of calculated cut-off and maximum transmission frequencies of the TE_{10} mode by considering: (a) cells, and (b) windows of RVC foams as rectangular waveguides.

Figure 13: Reflection coefficient of CVC foams, whose bulk densities are given in the legend, between 1.5 and 20 THz.